Quadrature Method of Moments for Population-Balance Equations

Daniele L. Marchisio, Jesse T. Pikturna, Rodney O. Fox, and R. Dennis Vigil
Dept. of Chemical Engineering, Iowa State University, Ames, IA 50011

Antonello A. Barresi
Dip. Scienza dei Materiali ed Ingegneria Chimica, Politecnico di Torino, C.so Duca degli Abruzzi 24, 10129, Torino, Italy

Although use of computational fluid dynamics (CFD) for simulating precipitation (and particulate systems in general) is becoming a standard approach, a number of issues still need to be addressed. One major problem is the computational expense of coupling a standard discretized population balance (DPB) with a CFD code, as this approach requires the solution of an intractably large number of transport equations. In this work the quadrature method of moments (QMOM) is tested for size-dependent growth and aggregation. The QMOM is validated by comparison with both Monte Carlo simulations and analytical solutions using several functional forms for the aggregation kernel. Moreover, model predictions are compared with a DPB to compare accuracy, computational time, and the number of scalars involved. Analysis of the relative performance of various methods for treating aggregation provides readers with useful information about the range of application and possible limitations.

Introduction

Precipitation and crystallization are widely studied problems in modern chemical engineering. Several phenomena are involved, such as mixing at various scales, nucleation, crystal growth, aggregation, and breakage. The influence of mixing on this kind of process has been studied for more than two decades, leading to different and sometimes contradictory results (Baldyga et al., 1995; Barresi et al., 1999; Kim and Tarbell, 1996). The final crystal-size distribution (CSD), as well as crystal morphology (Pagliolico et al., 1999; Jung et al., 2000) are strongly influenced by local concentrations and then by mixing if the process is very fast. Moreover, mixing also plays an important role in determining particle interactions (Krutzer et al., 1995; Zauner and Jones, 2000; Sung et al., 2000).

Since the process is complicated by the interaction of the mechanisms involved, it is difficult and sometimes impossible to propose scale-up and design rules from experimental data. Thus, a modeling approach provides a useful tool for interpreting experimental data. The model has to be as accurate and complete as possible with respect to the two key phenomena involved: mixing and solids evolution. The first aspect has been recently handled by computational fluid dynamics (CFD) coupled with a micromixing model (Baldyga and Orciuch, 2001; Marchisio et al., 2001; Piton et al., 2000). In these articles the role of mixing at all scales is modeled and explained, and the solids evolution is modeled with the standard moment method (SMM). This method is based on the idea of tracking only the moments of the CSD, rather than the entire CSD. However, the transport equations of the moments need to be written in a closed form, namely, in terms of the moments themselves. An up-to-date description of the possible approaches has been recently published by Diemer and Olson (2002), whereas a simplified approach for simultaneous nucleation, molecular growth, and aggregation has been implemented by Marchisio et al. (2002) for CFD calculations.

Other possible approaches for the solution of the population-balance equation are based on the discretization of the particle internal coordinate(s), leading to a discretized population balance (DPB). Depending on the philosophy of this discretization, different methods have been developed for aggregation and breakage (Kumar and Ramkrishna, 1996a,b;

Correspondence concerning this article should be addressed to D. L. Marchisio.

Vanni, 1999) and aggregation and crystal growth (Marchal et al., 1988; Muhr et al., 1996; Litster et al., 1995; Hounslow et al., 1988). Another completely different approach is based on Monte Carlo methods, in which a population of particles is considered and undergoes a birth–death process (Smith and Matsoukas, 1998). A review of the state of the art of population balances limited to the aggregation-breakage problem can be found in Ramkrishna (1985), whereas in Vanni (2000) a detailed comparison of different methods is studied and discussed. A recent comprehensive treatment of population balances can be found in Ramkrishna (2000).

In general, the DPB approach describes the population balance accurately, but can involve an extremely high number of scalars. If the final application is the implementation of the population balance in a CFD code, then the solution of the scalars has to be done in every cell of the computational domain, resulting in a very high calculation time and memory problems. Thus, in order to study the effects of mixing using CFD, it will be necessary to develop alternative approaches that have nearly the same accuracy as the DPB approach, but use fewer scalars.

One such approach is the quadrature method of moments (QMOM), first proposed by McGraw (1997) for studying size-dependent growth in aerosols and then applied to aggregation problems by Barrett and Webb (1998). The method has been extended by Wright et al. (2001) to treat a bivariate aerosol distribution. In this article the QMOM approach is tested for solving the length-based population-balance equation for molecular growth and aggregation. The aim of this work is to show that this method has an accuracy of the same order of magnitude as the DPB approaches available in the literature for simultaneous nucleation, growth, and aggregation, but with a drastic reduction in the number of the scalars involved. Several cases are investigated in order to illustrate the advantages and the limitations of the QMOM approach.

Population Balance

The population balance is a continuity statement based on the number density function. This function is defined in several ways depending on the properties of the system under observation. Given the coordinates of the property vector $\boldsymbol{\xi} \equiv (\xi_1, \ldots, \xi_n)$ that specify the state of the particle, the number density function $n(\boldsymbol{\xi}; \boldsymbol{x}, t)$ is defined as follows

$$n(\xi_1, \ldots, \xi_n; \boldsymbol{x}, t)d\xi_1, \ldots, d\xi_n = n(\boldsymbol{\xi}; \boldsymbol{x}, t)\, d\boldsymbol{\xi} \quad (1)$$

and represents the number of particles with a value of the property vector between $\boldsymbol{\xi}$ and $\boldsymbol{\xi} + d\boldsymbol{\xi}$. For an *inhomogeneous* particulate system the governing equation is (Randolph and Larson, 1988)

$$\frac{\partial n(\boldsymbol{\xi}; \boldsymbol{x}, t)}{\partial t} + \langle u_i \rangle \frac{\partial n(\boldsymbol{\xi}; \boldsymbol{x}, t)}{\partial x_i} - \frac{\partial}{\partial x_i}\left[\Gamma_t \frac{\partial n(\boldsymbol{\xi}; \boldsymbol{x}, t)}{\partial x_i}\right] = -\frac{\partial}{\partial \xi_j}\left[n(\boldsymbol{\xi}; t)\zeta_j\right] + h(\boldsymbol{\xi}; t) \quad (2)$$

where repeated indices imply summation and where $\langle u_i \rangle$ is the Reynolds-average velocity in the ith direction, x_i is the spatial coordinate in the ith direction, and Γ_t is the turbulent diffusivity. The "flux in $\boldsymbol{\xi}$-space" is denoted by

$$\zeta_j \equiv \frac{d\xi_j}{dt} \qquad j \in 1, \ldots, N \quad (3)$$

and $h(\boldsymbol{\xi}; t)$ represents the net rate of introduction of new particles into the system (Hulburt and Katz, 1964). Notice that Eq. 2 is usually implemented in CFD codes by means of user-defined scalars. By using this approach, the CFD code solves the transport equations for a number of scalars defined by the user. The CFD code handles the lefthand side of the equation (that is, it handles convection and turbulent diffusion), and the problem is, thus, reduced to the formulation of the source term in an acceptable manner (that is, the source term on the righthand side of Eq. 2). Since this work focuses on the closure problem related to the source term of the population balance, hereinafter, only the homogeneous cases will be considered. Extension to inhomogeneous cases then follows the methods used in our earlier work (Marchisio et al., 2002).

Depending on the system of interest, the number density function $n(\boldsymbol{\xi}; t)$ may have only one internal coordinate (such as particle length or volume), or multiple coordinates (such as particle volume and surface area). Usually when dealing with nucleation and growth problems, the internal coordinate is a characteristic length, whereas when dealing with aggregation and breakage, the internal coordinate is the particle volume. In this work, we will consider a number density function defined in terms of the particle length ($\xi_1 \equiv L$), and then the homogeneous population balance is

$$\frac{\partial n(L; t)}{\partial t} = -\frac{\partial}{\partial L}\left[G(L)n(L; t)\right] + B(L; t) - D(L; t) \quad (4)$$

where $G(L)$ is the growth rate, and $B(L; t)$ and $D(L; t)$ are, respectively, the birth and the death rates due to aggregation.

The study of aggregation started from the work of Smoluchowski (1917), who first defined the birth and death rates for a discrete system composed of interacting monomers. The equations can be rewritten for a continuous system in terms of the particle volume (v) as follows

$$B'(v; t) = \frac{1}{2}\int_0^v \beta'(v - \epsilon, \epsilon)n'(v - \epsilon; t)n'(\epsilon; t)d\epsilon \quad (5)$$

and

$$D'(v; t) = n'(v; t)\int_0^\infty \beta'(v, \epsilon)n'(\epsilon, t)\, d\epsilon \quad (6)$$

where $n'(v; t)$ is the particle number density with particle volume as internal coordinate, and $\beta'(v, \epsilon)$ is the corresponding aggregation kernel. The latter is a measure of the frequency of the collision of particles of volume v and ϵ that are successful in producing a particle of volume $v + \epsilon$.

In order to introduce these terms in Eq. 4, one further operation is needed. Assuming that length and volume are related by $v \propto L^3$, it is easily shown that Eqs. 5 and 6 ex-

pressed in a length-based form are as follows

$$B(L;t)=\frac{L^2}{2}\int_0^L \frac{\beta\left[(L^3-\lambda^3)^{1/3},\,\lambda\right]}{(L^3-\lambda^3)^{2/3}} \times n\left[(L^3-\lambda^3)^{1/3};\,t\right]n(\lambda;t)\,d\lambda \quad (7)$$

and

$$D(L;t)=n(L;t)\int_0^\infty \beta(L,\,\lambda)n(\lambda;t)d\lambda \quad (8)$$

where L and λ are the dimensions of the particles with volumes v and ϵ, respectively. A detailed derivation of these equations can be found in Marchisio et al. (2003a).

Vanni (2000) reviewed several methods for solving population-balance equations, focusing in particular on aggregation–breakage problems. Likewise, Ramkrishna (2000) presents a lucid explanation of the mathematical issues involved. As explained in the introduction, the most common approach is the DPB, based on the discretization of the particle coordinate (such as particle volume or length). The available methods for aggregation–breakage problems basically differ on the discretization used, but in general nonlinear discretization is used. The situation is completely different for cases with crystal growth, not only because the problem is formulated using particle length as the internal coordinate, but also because in this case a linear discretization is the best approach.

Standard moment method

A computationally attractive alternative approach is the SMM in which the key is the formulation of the problem in terms of the lower-order moments in closed form (that is, involving only functions of the moments themselves). For a homogeneous system, the kth moment is defined by

$$m_k(t)=\int_0^\infty L^k n(L;t)\,dL \quad (9)$$

The first five moments ($k \in 0,\,\ldots,\,4$) are of particular interest, since they are related to the total number particle density ($N_t=m_0$), the total particle area ($A_t=k_a m_2$), and the total solids volume ($V_t=k_v m_3$) by shape factors ($k_a,\,k_v$) that depend on particle morphology. Moreover, using this approach a mean crystal size can be defined as follows

$$d_{43}=\frac{m_4}{m_3} \quad (10)$$

and the solids concentration is given by

$$c_s=\frac{\rho k_v m_3}{M} \quad (11)$$

where ρ is the crystal density, k_v is the volume shape factor, and M is the molecular weight of the crystal.

In a homogeneous system, the resulting transport equation for the kth moment is as follows

$$\frac{dm_k(t)}{dt}=(0)^k J(t)+\int_0^\infty kL^{k-1}G(L)n(L;t)\,dL + \overline{B}_k(t)-\overline{D}_k(t) \quad (12)$$

where $J(t)$ is the nucleation rate and the last two terms represent the effects of birth and death, respectively, due to aggregation. The first of these can be rewritten by setting $u^3=L^3-\lambda^3$ and reversing the order of integration (Litster et al., 1995)

$$\overline{B}_k(t)=\frac{1}{2}\int_0^\infty n(\lambda;t)\int_0^\infty \beta(u,\,\lambda)(u^3+\lambda^3)^{k/3}n(u;t)\,du\,d\lambda \quad (13)$$

whereas the second one is

$$\overline{D}_k(t)=\int_0^\infty L^k n(L;t)\int_0^\infty \beta(L,\,\lambda)n(\lambda;t)\,d\lambda\,dL \quad (14)$$

In the case of size-independent growth (G function of time only) and without aggregation and breakage ($\overline{B}_k$ and $\overline{D}_k$ null), the moments can be computed directly without requiring additional knowledge of the number density function. In all the other cases SMM is applicable under particular simplifications (Marchisio et al., 2002) or using the closure proposed by Diemer and Olson (2002).

Quadrature Method of Moments

The QMOM can be thought of as a particular class of moment method where the closure problem is solved by using a quadrature approximation (McGraw, 1997)

$$n(L;t)\approx\sum_{i=1}^{N_q} w_i(t)\,\delta\left[L-L_i(t)\right] \quad (15)$$

so that, for example

$$m_k(t)\approx\sum_{i=1}^{N_q} w_i(t)L_i^k(t) \quad (16)$$

The essence of this method is the fact that the abscissas $L_i(t)$ and the weights $w_i(t)$ can be specified from the lower-order moments. In fact, in order to build a quadrature approximation of order N_q, it suffices to know the first $2N_q$ moments. Thus, for example, the first six moments ($m_0,\,\ldots,\,m_5$) suffice to build a QMOM approximation of order $N_q=3$. Note that Eq. 15 provides a rough approximation of the CSD. Although limited, this information can be useful for a qualitative comparison with experimental CSDs.

Once abscissas and weights have been computed, any integral involving the number distribution function ($n(L;\,t)$) can be approximated using Eq. 15. The procedure used to find w_i and L_i from the moments is the so-called product-difference

(PD) algorithm proposed by Gordon (1968), and based on the theory of canonical moments (Dette and Studden, 1997). The first step is the construction of a matrix $\boldsymbol{P}$, with components $P_{i,j}$ starting from the moments (McGraw, 1997). The components in the first column of $\boldsymbol{P}$ are

$$P_{i,1} = \delta_{i1} \qquad i \in 1, \ldots, 2N_q + 1 \tag{17}$$

where δ_{i1} is the Kronecker delta. The components in the second column of $\boldsymbol{P}$ are

$$P_{i,2} = (-1)^{i-1} m_{i-1} \qquad i \in 1, \ldots, 2N_q + 1 \tag{18}$$

Since the final weights can be corrected by multiplying by the true m_0, the calculations can be done assuming a normalized distribution (that is, $m_0 = 1$). Then the remaining components are found from the PD algorithm

$$P_{i,j} = P_{1,j-1}P_{i+1,j-2} - P_{i,j-2}P_{i+1,j-1} \qquad j \in 3, \ldots, 2N_q + 1 \quad \text{and} \quad i \in 1, \ldots, 2N_q + 2 - j \tag{19}$$

If, for example, $N_q = 2$, then $\boldsymbol{P}$ becomes

$$\boldsymbol{P} = \begin{bmatrix} 1 & 1 & m_1 & m_2 - m_1^2 & m_3 m_1 - m_2^2 \\ 0 & -m_1 & -m_2 & -m_3 + m_2 m_1 & 0 \\ 0 & m_2 & m_3 & 0 & 0 \\ 0 & -m^3 & 0 & 0 & 0 \\ 0 & 0 & 0 & 0 & 0 \end{bmatrix} \tag{20}$$

The coefficients of the continued fraction (α_i) are generated by setting the first element equal to zero ($\alpha_1 = 0$), and computing the others according to the following recursive relationship

$$\alpha_i = \frac{P_{1,i+1}}{P_{1,i}P_{1,i-1}} \qquad i \in 2, \ldots, 2N_q \tag{21}$$

A symmetric tridiagonal matrix is obtained from sums and products of α_i

$$a_i = \alpha_{2i} + \alpha_{2i-1} \qquad i \in 1, \ldots, 2N_q - 1 \tag{22}$$

and

$$b_i = -\sqrt{\alpha_{2i+1} + \alpha_{2i-1}} \qquad i \in 1, \ldots, 2N_q - 2 \tag{23}$$

where a_i and b_i are, respectively, the diagonal and the codiagonal of the Jacobi matrix. Once the tridiagonal matrix is determined, generation of the weights and abscissas is done by finding its eigenvalues and eigenvectors. In fact, the eigenvalues are the abscissas, and the weights can be found as follows

$$w_j = m_0 v_{j1}^2 \tag{24}$$

where v_{j1} is the first component of the jth eigenvector $\boldsymbol{v}_j$.

Use of QMOM for modeling time evolution of particulate systems requires the solution of a system of ordinary differential equations (ODE) and the solution of the eigenvalues problem. The former was handled by using the ODE package ODEPACK (LSODE Fortran double-precision subroutine), whereas for the latter the linear algebra package EISPACK (IMTQL2 Fortran double-precision subroutine) was used. For details see Press et al. (1992).

When working with the first six moments ($m_0, \ldots, m_5$), the method is based on the approximation of the number density function by a sum of $N_q = 3$ delta functions

$$n(L;t) = w_1(t)\,\delta[L - L_1(t)] + w_2(t)\,\delta[L - L_2(t)] + w_3(t)\,\delta[L - L_3(t)] \tag{25}$$

and represents a population made up of three classes of particles with dimension $L_1(t)$, $L_2(t)$, and $L_3(t)$ and number densities $w_1(t)$, $w_2(t)$, $w_3(t)$. As an example, consider a population with $L_1(0) = 1$, $L_2(0) = 2$, $L_3(0) = 3$ m, $w_1(0) = 0.2$, $w_2(0) = 0.1$, and $w_3(0) = 0.7$, and with a constant growth rate $G = 1\ \text{ms}^{-1}$. The moment equations for this system are

$$\frac{dm_k}{dt} = kGm_{k-1} \qquad k \in 0, \ldots, 5 \tag{26}$$

with initial conditions

$$m_k(0) = \sum_{i=1}^{3} w_i(0) L_i(0)^k \qquad k \in 0, \ldots, 5 \tag{27}$$

From the first six moments ($m_0, \ldots, m_5$), the PD algorithm can be used to compute the three weights and three abscissas. Results are reported in Figure 1, where it is shown that $w_i(t)$ remains constant, whereas $L_i(t)$ increases following the real increase in length of the three classes.

For the case where $L_1(0) = 2$, $L_2(0) = 3$, and $L_3(0) = [L_1(0)^3 + \mathrm{L}_2(0)^3]^{1/3}$ and $w_1(0) = 0.5$, $w_2(0) = 0.5$, $w_3(0) = 0.0$, and particles L_1 aggregate with particles L_2 to give particles L_3 preserving the volume (without nucleation and growth), the source terms for aggregation are very simple and the population balance written in terms of the moments is as follows

$$\frac{dm_k(t)}{dt} = \left(-L_1(t)^k - L_2(t)^k + L_3(t)^k\right)\left[m_0(t) - \frac{m_0(0)}{2}\right] \qquad k = 0, \ldots, 5. \tag{28}$$

Supposing an aggregation rate of $[m_0(t) - m_0(0)/2]$ and again tracking abscissas and weights by using the PD algorithm, three different eigenvalues equal to $L_1(t) = 2$, $L_2(t) = 3$, $L_3(t) = (L_1(t)^3 + L_2(t)^3)^{1/3}$ and the three weights reported in Figure 2 are found. As can be seen, $w_1(t)$ and $w_2(t)$ go to zero and $w_3(t)$ goes to 0.5. In fact, the total number of particles is one half after all particles of dimension $L_1(t)$ and $L_2(t)$ have aggregated. Obviously, anytime the moments refer to a number density function that cannot be exactly represented by three classes of particles, Eq. 25 is no longer exact. For these cases, validation of the method is required.

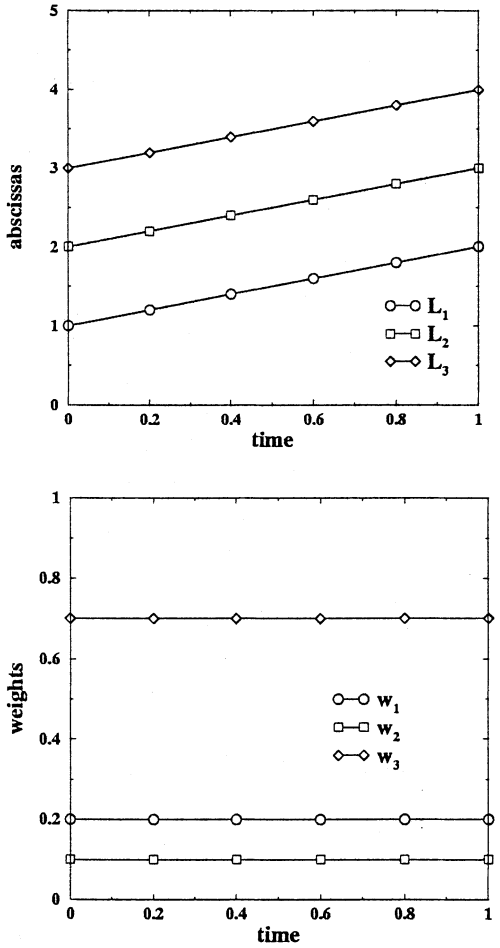

Figure 1. Evolution with time of the abscissas (L_i) and weights (w_i) for three classes of particles in the case of size-independent growth and no aggregation.

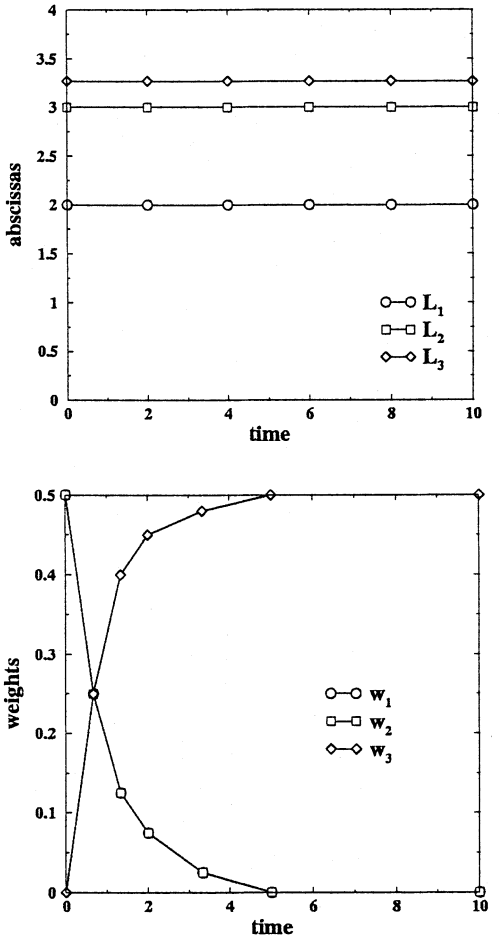

Figure 2. Evolution with time of the abscissas (L_i) and weights (w_i) for three classes of particles with aggregation and no growth.

Other Approaches: Monte Carlo and DPB Methods

In part of the investigated cases Monte Carlo (MC) simulations of the population balance were used to validate the QMOM results.

The constant-number method of Smith and Matsoukas (1998) was used as a model for these simulations. When this method is applied, the number of particles in the system remains constant. Because aggregation processes result in a net loss of particles, the system volume is increased in order to keep m_0 constant, and the time increment is adjusted appropriately. In the method, an initial distribution of particles is specified. Two randomly selected particles (indicated with i and j) are tested for an aggregation event. An aggregation event may occur with probability equal to

$$p_{ij} = \frac{k_{ij}}{k_{\max}} \tag{29}$$

where p_{ij} is the aggregation probability for the couple of particles i and j, k_{ij} is the dimensionless aggregation kernel, and $k_{\max}$ is the maximum value of the aggregation kernel among all the particles. Note that in the case of aggregation with a constant kernel $p_{ij} = 1$. If an aggregation event occurs, the mass of the new particle is equivalent to the sum of the masses of the original two. The new particle replaces one of the two aggregated particles in the distribution, and a void is formed in place of the other. This void is filled by a replicate of a randomly selected particle from the current distribution. If an aggregation event does not occur, two new particles are chosen and tested. The appropriate time step (Δt_κ) for this aggregation event is then calculated based on the following

$$\Delta t_\kappa = \frac{\Delta C_\kappa}{z_\kappa \Sigma_l R_l} \tag{30}$$

where ΔC_κ is the change in the total number density due to that event, z_κ is the stoichiometric coefficient for the event, and R_l is the rate of event l per unit time and unit volume. Note that for binary aggregation $z_\kappa = -1$. Two new particles are then selected, and the entire process is repeated until the desired intensity of aggregation is obtained. Further details can be found in Smith and Matsoukas (1998).

The QMOM predictions were also compared with a specific DPB method for simultaneous nucleation, growth, and aggregation. For this purpose the DPB approach proposed by Litster et al. (1995) was employed. The latter was chosen from among those approaches that can model simultaneous nucleation, growth, and aggregation. For this reason, the model is simpler and less accurate than more rigorous approaches that are able to model only aggregation, and in some cases, breakage. The approach is based on Hounslow's idea that aggregates are formed of particles of 2^{i-1} monomers (as if only particles made by 1,2,4,8, … monomers exist). In terms of length-based expressions, this becomes $L_{i+1} = L_i 2^{1/3}$. More recently, a revised version of the model has been proposed, in which the discretization can be adjusted by means of a parameter, q. In this case, the discretization scheme becomes $L_{i+1} = L_i(2^{1/q})^{1/3}$ [see Hounslow et al. (1988) and Litster et al. (1995) for details].

Results and Discussion

The validation of the QMOM has been done in three steps. In the first two steps the ability of the QMOM to model crystal growth with size-independent and size-dependent growth rates was verified. In the third step, the ability of QMOM to predict aggregation using realistic aggregation kernels was investigated. In some cases and with the proper choice of the initial distribution, it was possible to compare the QMOM predictions with analytical solutions, but in other cases (that is, aggregation with Brownian and hydrodynamic kernels), it was necessary to use alternative approaches. In this work the constant-number Monte Carlo method proposed by Smith and Matsoukas (1998) was used and considered to be an accurate solution. Eventually a comparison with the DPB method was also perfomed.

Size-independent growth rate

For this case, moment equations can be expressed in closed form

$$\frac{dm_k}{dt} = kGm_{k-1} \qquad k \in 0, \ldots, 5 \tag{31}$$

and the system is represented by an analytical solution. The solution of the system obtained by using the moments recalculated from the quadrature approximation, was found in excellent agreement with the analytical solution, proving that the abscissas and weights obtained from the PD algorithm are able to give back the exact values of the moments. Different initial CSDs were used such as Dirac-delta and step functions. In Figure 3 the first six normalized moments are reported for the following initial CSD

$$n(L) = 3L^2 \frac{N_o}{v_o} \exp\left(-L^3/v_o\right) \tag{32}$$

where $N_o = 1\ \mathrm{m}^{-3}$, $v_o = 1\ \mathrm{m}^{-3}$, $G = G_o = 1.0\ \mathrm{ms}^{-1}$. The results show that the total number density is constant, whereas m_1 varies linearly. For all the moments the agreement between the analytical solution and the solution found with the PD algorithm was excellent.

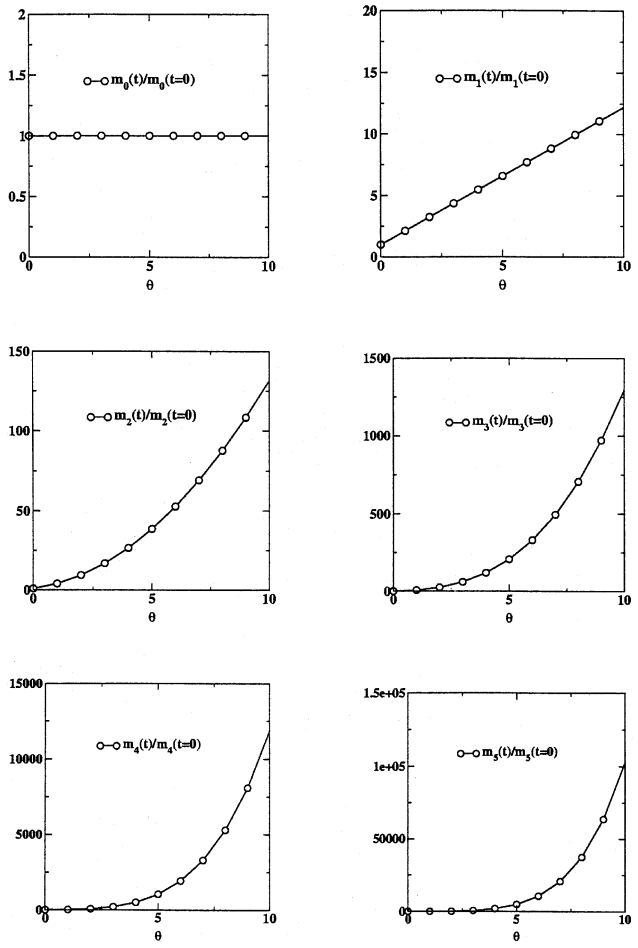

Figure 3. Evolution vs. dimensionless time ($\theta = tG_o/v_o^{1/3}$) of the first six moments for size-independent growth.

The reported, results are obtained by using QMOM. The analytical solution is not reported, since perfect overlapping was found.

Size-dependent growth rate

For this case, by using the QMOM, the problem is formulated in closed form

$$\frac{dm_k}{dt} = \int_0^\infty kG(L)n(L;t)L^{k-1}dL \approx k\sum_{i=1}^{3} G\left[L_i(t)\right]L_i(t)^{k-1}w_i(t) \qquad k \in 0, \ldots, 5 \tag{33}$$

McGraw (1997) showed that QMOM is able to correctly predict the first six moments for a growth law of the form

$$G(L) = \frac{G_o}{L} \tag{34}$$

From his calculations, the error was estimated to be lower than 0.1%. In this work a comparison is made by using the same initial condition as in the previous case and $G_o = 1.0$

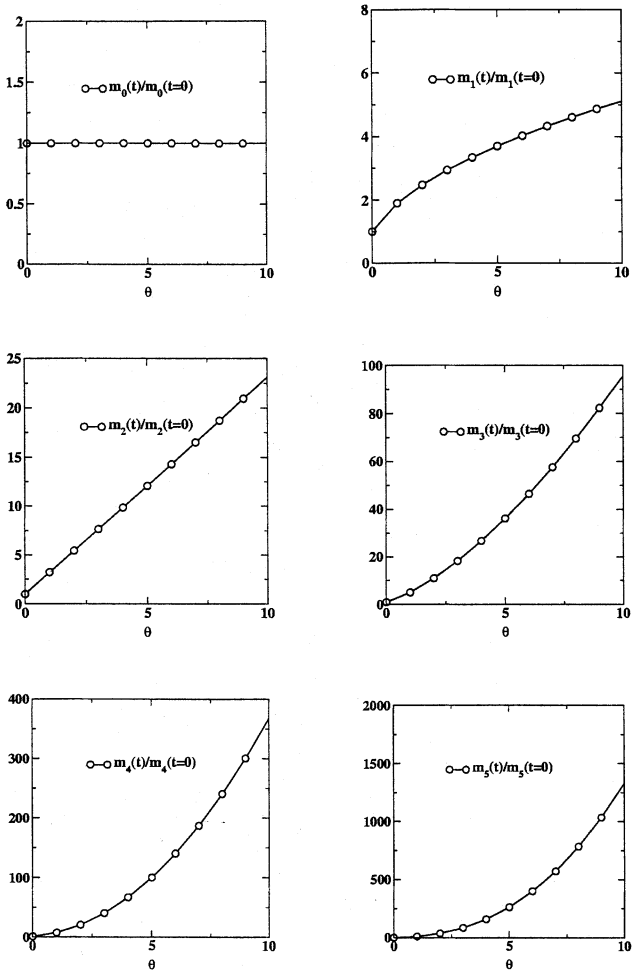

Figure 4. Evolution vs. dimensionless time ($\theta = tG_o/v_o^{2/3}$) of the first six moments for size-dependent growth.

The reported results are obtained by using QMOM. The analytical solution (available for even moments) is not reported, since perfect overlapping was found.

m^2s^{-1}. Results from QMOM were compared with analytical solutions, which are available only for even moments, for example

$$\frac{dm_2}{dt} = 2G_o m_0 \tag{35}$$

In Figure 4 the first six moments are reported against time. As is possible to see, $m_0(t)$ is again constant, whereas in this case $m_2(t)$ varies linearly with time. Also in this case excellent agreement was found with a maximum error of 0.3%. In general for problems involving only growth, we have observed excellent agreement between QMOM and methods that account for the entire CSD.

Aggregation

Using QMOM for the aggregation terms in Eq. 12, the moment equations become

$$\frac{dm_k}{dt} = \frac{1}{2}\int_0^\infty n(\lambda; t)\int_0^\infty \beta(\lambda, u)(u^3 + \lambda^3)^{k/3} n(u; t)\, du\, d\lambda$$

$$- \int_0^\infty L^k n(L; t)\int_0^\infty \beta(L, \lambda) n(\lambda; t)\, d\lambda\, dL \tag{36}$$

$$\approx \frac{1}{2}\sum_{i=1}^{3} w_i \sum_{j=1}^{3} w_j \beta(L_i, L_j)\left(L_i^3 + L_j^3\right)^{k/3} \tag{37}$$

$$- \sum_{i=1}^{3} w_i L_i^k \sum_{j=1}^{3} w_j \beta(L_i, L_j) \qquad k \in 0, \ldots, 5 \tag{38}$$

Validation of the QMOM was carried out first by comparison with analytical solutions. In fact, the initial CSD reported in Eq. 32 provides analytical solutions in a number of cases (Gelbard and Seinfield, 1978).

In this work, the QMOM was validated for four different kernels

(1) Constant

$$\beta(L, \lambda) = \beta_0 \tag{39}$$

(2) Sum

$$\beta(L, \lambda) = \beta_0(L^3 + \lambda^3) \tag{40}$$

(3) Brownian

$$\beta(L, \lambda) = \beta_0 \frac{(L + \lambda)^2}{L\lambda} \tag{41}$$

(4) Hydrodynamic

$$\beta(L, \lambda) = \beta_0(L + \lambda)^3 \tag{42}$$

Note that analytical solutions are available for kernels 1 and 2 (Gelbard and Seinfield, 1978). As concerns MC simulations, in this work the method proposed by Smith and Matsoukas (1998) is extended to predict size distributions resulting from the aggregation of particles driven by the sum and hydrodynamic kernels.

For the constant kernel with an exponential initial CSD (Eq. 32), the moments evolve as follows

$$m_k(t) = m_k(t=0)\left(\frac{2}{2 + N_o \beta_0 t}\right)^{1 - k/3} \tag{43}$$

In our calculations we considered $N_o = 1\ \mathrm{m}^{-3}$, $v_o = 1\ \mathrm{m}^3$, and $\beta_0 = 1\ \mathrm{m}^3 \cdot \mathrm{s}^{-1}$. The evolution of the moments is reported in Figure 5. Results clearly show that m_3 remains constant, since during aggregation total particle volume is conserved. The moments of the order lower than three decrease, whereas the others increase. In the case under investigation, the QMOM was found to be in excellent agreement with the analytical solution and the Monte Carlo simulations.

Concerning MC simulations, the effect of the number of particles used in the simulation of the statistical errors is very

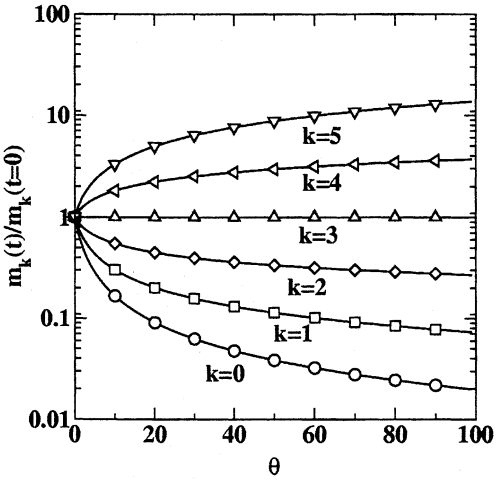

Figure 5. Normalized moments for aggregation with constant kernel ($\beta_0 = 1.0\ m^3 \cdot s^{-1}$) against the dimensionless time ($\theta = N_0 \beta_0 t$) (lines: analytical solution; symbols: QMOM predictions).

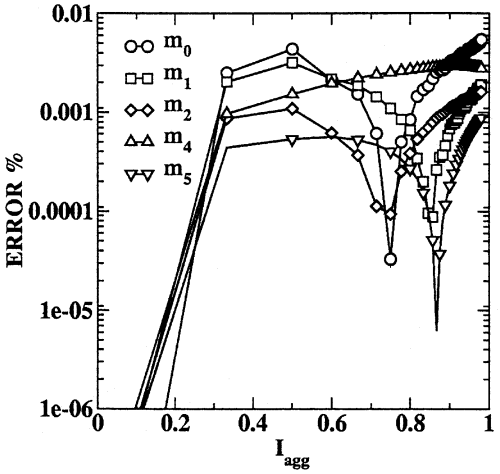

Figure 7. Percent error for the first six moments for aggregation with constant kernel ($\beta_0 = 1.0\ m^3 \cdot s^{-1}$).

In this case, the analytical solution is used to determine the error; m_3 is not reported, since the error is lower than $10^{-6}\%$.

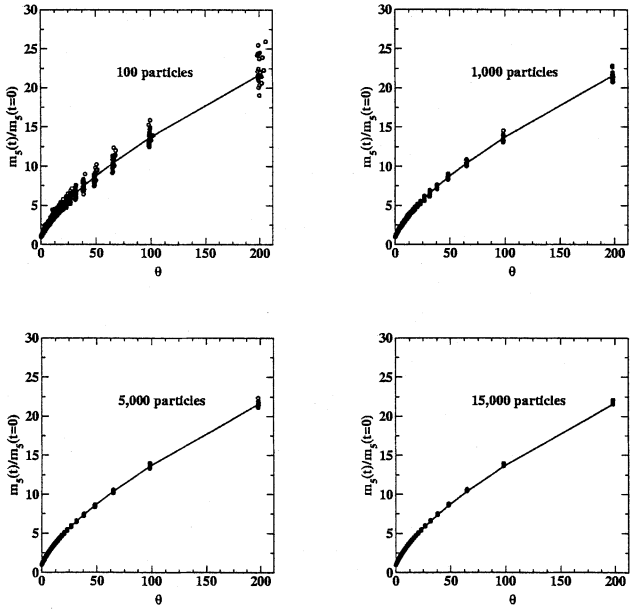

Figure 6. Comparison between analytical solution (continuous line) and Monte Carlo predictions (circles) for m_5 with different numbers of particles against the dimensionless time ($\theta = N_0 \beta_0 t$) (Monte Carlo predictions refer to 50 different realizations).

important. In Figure 6, fifty different realizations for m_5 against the dimensionless time ($\theta = N_0 \beta_0 t$) are reported and compared with the analytical solution. Each realization is a different random walk and represents a possible evolution of the particulate system. The comparison shows that, as the number of particles is increased, the different realizations collapse on the analytical solution, and moreover it confirms that 15,000 particles are enough to describe the particles' evolutions. Hereinafter, all the comparisons with MC simulations were run with a constant 15,000 particles.

In order to quantify the ability of the model to predict system properties, it is useful to define the intensity of aggregation (Ilievski and Hounslow, 1995)

$$I_{agg} = 1 - \frac{m_0(t)}{m_0(0)} \tag{44}$$

I_{agg} is 0 when the number of aggregation events is null, and goes to 1 as this number increases. In Figure 7 the error for QMOM relative to the exact solution is reported against I_{agg}. As can be seen, the error for all moments is less than 0.01%. Since the third moment is perfectly predicted, the relative error is not reported.

With the DPB method proposed by Hounslow, $i = 20$ classes are required to ensure the conservation of aggregate volume (that is, m_3 constant) for this example. For this value of i, the errors for moments with order lower than 3 were around 1% for I_{agg} approaching 1, whereas the fourth and fifth moments were around 6%. Only after adopting the modification proposed by Litster et al. (1995), with $q = 5$, are the errors comparable to those of the QMOM. Thus, for equivalent accuracy, the QMOM requires six scalars, while the DPB requires 100 for the constant kernel case.

If the same initial CSD is considered (Eq. 32) with the sum kernel, an analytical solution also exists. For this case, Gelbart and Seinfield (1978) found the following population density function ($N_o = 1\ m^{-3}$, $v_o = 1\ m^3$, and $\beta_0 = 1\ s^{-1}$)

$$n(L;t) = \frac{3(1-T)}{L\sqrt{T}} \exp\left[-(1+T)L^3\right] I_1\left(2L^3\sqrt{T}\right) \tag{45}$$

where $T = [1 - \exp(-t)]$ and I_1 is the modified Bessel function of the first kind of order one. Numerical integration [using the function BESSE1 to evaluate the Bessel function

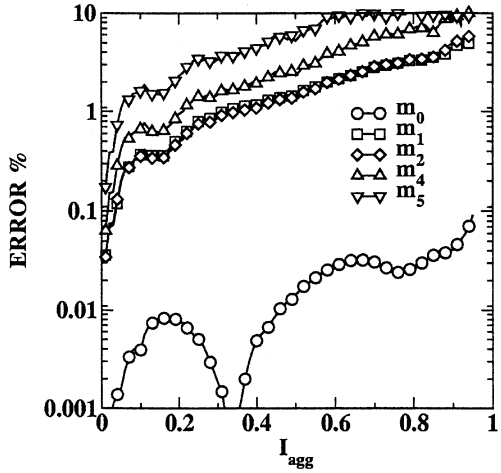

Figure 8. Percent error for the first six moments for aggregation with sum kernel ($\beta_0 = 1.0\ s^{-1}$).

In this case, the analytical solution is used to determine the error; m_3 is not reported, since the error is lower than $10^{-6}\%$.

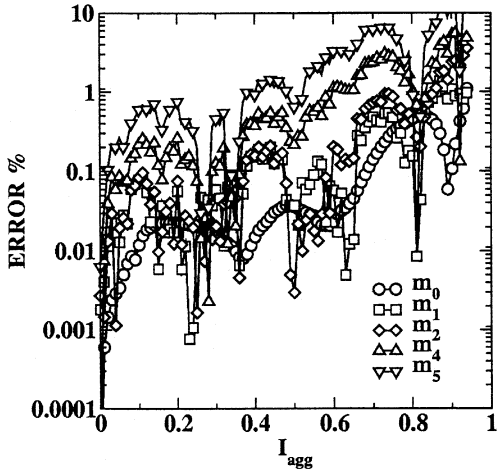

Figure 10. Percent error for the first six moments for aggregation with hydrodynamic kernel ($\beta_0 = 1.0\ s^{-1}$).

The Monte Carlo solution is used to determine the error; m_3 is not reported, since the error is lower than $10^{-6}\%$.

(Press et al., 1992)] gives the moment evolutions. In Figure 8 the errors found using the QMOM are calculated relative to the analytic solution. Again, excellent agreement was found between QMOM, the analytic solution, and MC simulations. In this case, the comparison was done with MC simulations using 15,000 particles.

For the sum kernel, errors for moments of order lower than 3 are always less than 5% and the third moment is perfectly predicted. For m_4 and m_5 errors are less than 7% for I_{agg} smaller than 0.5, and for I_{agg} close to unity are equal to about 9% and 10%, respectively.

In comparison, the DPB errors with $i = 30$ classes are quite high and vary from 20% for m_0 to 300% for m_5. If Litster's modification is applied, the errors are comparable to those obtained with the QMOM only if $q = 6$. Thus, for equivalent accuracy, the QMOM requires six scalars, while the DPB requires 180 for the sum kernel case.

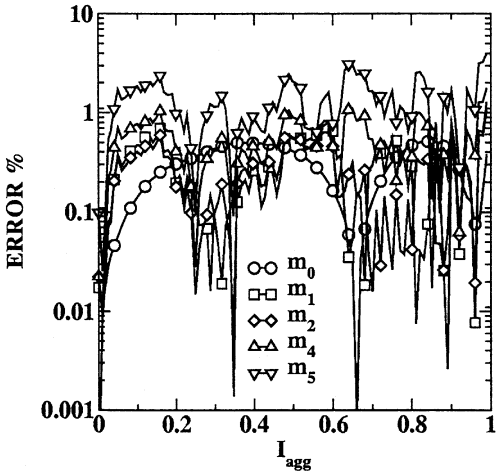

Figure 9. Percent error for the first six moments for aggregation with Brownian kernel ($\beta = 1.0\ m^3 \cdot s^{-1}$).

The Monte Carlo solution is used to determine the error; m_3 is not reported since the error is lower than $10^{-6}\%$.

For Brownian aggregation, QMOM predictions were compared with those of MC simulations (see Figure 9). Also in this case MC simulations were run with 15,000 particles. The agreement between the two methods is excellent. The third moment is perfectly predicted, whereas for moments of order lower than 4, the errors are less than 1%. Only for m_5 is the error greater than 1%, but still less than 3%. It is interesting to note here that m_5 is calculated only because it is needed in the PD algorithm. In fact, the highest-order moment that is used for comparison with the experimental data is m_4 (Eq. 10), for which the error is less than 1%. Moreover, results confirm that in this case Brownian aggregation can be treated with the constant kernel; in fact, under the hypothesis of aggregating particles of the same size

$$\beta(L, \lambda) = \beta_0 \frac{(L + \lambda)^2}{L\lambda} \approx 4\beta_0 \tag{46}$$

The errors found using the DPB are, thus, similar to those reported earlier for the constant kernel.

QMOM errors are reported in Figure 10 for the hydrodynamic kernel. Again, the agreement between QMOM and Monte Carlo simulations is surprisingly good. Also in this case Monte Carlo simulations were run with 15,000 particles. For m_0, the error is always less than 1%, and for m_1 and m_2, it is of the same order of magnitude. As in the other cases, m_3 is perfectly predicted, whereas the errors for m_4 and m_5 are larger. However, for I_{agg} less than 0.9, errors are relatively small, and only when I_{agg} exceeds 0.9 are errors greater than 5% but still lower than 10%. Comparison with DPB showed that only by using $i = 30$ classes and $q = 5$ are the errors of the same order of magnitude as QMOM for the hydrodynamic kernel.

Besides the exponential distribution, other initial CSDs were considered, such as a monomodal and bimodal step distribution. The agreement between the QMOM and the MC simulation was excellent in all the cases investigated.

It also is very interesting to investigate the effect of the number of nodes in the quadrature approximation. When QMOM predictions with two, three, and four nodes were compared, it was observed that increasing the number of nodes leads to a small improvement in QMOM predictions. However, the order of magnitude of the errors was very similar. A detailed description of the effect of the number of nodes on the overall accuracy of the method has been reported elsewhere (Marchisio et al., 2003a). Results showed that three nodes offer the best trade-off between number of scalars and accuracy.

The validation process leads us to the conclusion that the reduction in the number of scalars to be tracked is drastic in comparison with standard DPB methods (from 50–200 to 6). This drastic reduction of scalars does not come with a loss of accuracy, but has a strong impact on the CPU time. It is important to highlight here that for CFD applications the number of scalars is of primary importance. For these simulations, in fact, the controlling time is very often constituted by the solution of the convection and diffusion terms (see Eq. 2), and a system with 50–200 classes is intractable for a real geometry, whereas six moments can be easily solved. Moreover, besides reducing the number of scalars, the QMOM solves more efficiently the set of equations; in fact, a reduction of the CPU is even detected in the homogeneous case. For example, for constant kernel working with the DPB with 20 classes, the CPU time is 0.04 s (452 calls for the ODE integrator), whereas for the QMOM with six moments, the CPU time is 0.01 s (163 calls for the ODE integrator). As can be easily calculated, using the QMOM reduces the time per scalar from 2 ms/scalar down to 1.6 ms/scalar. The difference is more evident for the sum kernel where the CPU time is reduced from 0.2 s (422 calls) down to 0.01 s (142 calls). The comparison shows that the CPU time per scalars is about 5 ms/scalars for the DPB (with 40 classes) vs. 1.6 ms/scalars for the QMOM (six moments).

In conclusion, the QMOM is very attractive in comparison with other approaches, because it requires the solution of a much smaller set of transport equations working with excellent accuracy. Moreover, besides requiring fewer equations, the CPU time per scalar is smaller than the investigated DPB method, highlighting the fact that the QMOM bypasses the stiffness resulting from the discretization of the population-balance equation. In addition, as mentioned earlier, the method proposed does not present the problem of fixing the intervals to be considered in the simulations. Thus, unlike the DPB approach, it can be used for different CSDs without any modification. It also should be mentioned that reliable techniques for reconstructing the CSD for the moments exist, and a detailed discussion can be found in Diemer and Olson (2002).

Conclusions

A novel method (QMOM) for the treatment of population balances has been validated for size-dependent growth rate and aggregation by comparison with direct methods. Results show the great potential of QMOM for use with CFD codes. Indeed, QMOM presents several important advantages relative to direct methods:

(1) Extremely low number of scalars
(2) Extremely low CPU time
(3) There is no lower and upper limit on the classes involved.

The ability of the model to simulate aggregation-breakage problems has been investigated, and results confirmed the numerous advantages of the method (Marchisio et al., 2003a). We have recently integrated the QMOM in a CFD-based simulation code (Fluent) for aggregation and breakage, and the direct formulation of the problem and its application to a real case (that is, fluidized beds) are under study. Results from these studies are reported elsewhere (Marchisio et al., 2003b).

Acknowledgments

The research has been partially supported by the Italian Ministry of the University and of the Scientific Research (MURST 40%—Multiphase reactors: hydrodynamics analysis and solid-liquid analysis) and by the U.S. Department of Energy. The authors also gratefully acknowledge Prof. D. E. Rosner for suggesting the use of the QMOM for aggregation applications.

Notation

a_i = components of the diagonal of the Jacobi matrix of dimension $2N_q - 1$
A_t = total particle area, m^2
b_i = components of the codiagonal of the Jacobi matrix of dimension $2N_q - 2$
$B(L; t)$ = birth rate due to aggregation, $m^{-4} \cdot s^{-1}$
$B'(L; t)$ = birth rate due to aggregation, $m^{-6} \cdot s^{-1}$
c_s = solid concentration, $kg \cdot m^{-3}$
$D(L; t)$ = death rate due to aggregation, $m^{-4} \cdot s^{-1}$
$D'(L; t)$ = death rate due to aggregation, $m^{-6} \cdot s^{-1}$
d_{43} = mean crystal size, m
$G(L)$ = crystal growth rate, ms^{-1}
G_o = constant appearing in the crystal growth-rate expression, $m^2 \cdot s^{-1}$
$h(\boldsymbol{\xi}; t)$ = rate of introduction of new particles
I_{agg} = intensity of aggregation defined in Eq. 44
$J(t)$ = nucleation rate, $m^{-3} \cdot s^{-1}$
k = moment order
k_a = area shape factor
k_B = Boltzmann constant, $kg \cdot m^2 \cdot s^{-2} \cdot K^{-1}$
k_v = volume shape factor
L = particle length, m
L_i = abscissas of the quadrature approximation, m
m_k = kth moment of number density function, m^{k-3}
M = molecular weight, $kg \cdot mol^{-1}$
$n(L; t)$ = length-based number density function, m^{-4}
$n'(v; t)$ = volume-based number density function, m^{-6}
N_o = initial total particle number density, m^{-3}
N_q = order of the quadrature approximation
N_t = total particle number density, m^{-3}
$\boldsymbol{P}$ = product difference matrix of order $(2N_q + 1) \times (2N_q + 1)$
q = Litster's parameter
T = parameter defined in Eq. 45
t = time, s
$u = (L^3 - \lambda^3)^{1/3}$ particle length, m
$\langle u_i \rangle$ = Reynolds-averaged fluid velocity in the ith direction, $m \cdot s^{-1}$
v = particle volume, m^3
v_o = monomer volume, m^3
$\boldsymbol{v}_j$ = jth eigenvector
V_t = total particle volume, m^3

w_i = weights of the quadrature approximation, m^{-3}
$\boldsymbol{x}$ = spatial coordinate

Greek letters

α_i = components of the continued fraction vector of dimension $2N_q$
β = length-based aggregation kernel, $m^3 \cdot s^{-1}$
β' = volume-based aggregation kernel, $m^3 \cdot s^{-1}$
β_0 = size-independent part of the length-based aggregation kernel
Γ_t = turbulent diffusivity, $m^2 \cdot s^{-1}$
ϵ = particle volume, m^3
θ = dimensionless time
λ = particle volume, m^3
$\boldsymbol{\xi}$ = property vector
ρ = solid density, $kg \cdot m^{-3}$

Literature Cited

Baldyga, J., and W. Orciuch, "Barium Sulphate Precipitation in a Pipe—An Experimental Study and CFD Modelling," *Chem. Eng. Sci.*, **56**, 2435 (2001).

Baldyga, J., W. Podgoroska, and R. Pohorecki, "Mixing-Precipitation Model with Application to Double Feed Semi-Batch Precipitation," *Chem. Eng. Sci.*, **50**, 1281 (1995).

Barresi, A. A., D. Marchisio, and G. Baldi, "On the Role of Micro- and Meso-Mixing in a Continuous Couette-Type Precipitator," *Chem. Eng. Sci.*, **54**, 2339 (1999).

Barrett, J. C., and N. A. Webb, "A Comparison of Some Approximate Methods for Solving the Aerosol General Dynamic Equation," *J. Aerosol Sci.*, **29**, 31 (1998).

Dette, H., and W. J. Studden, *The Theory of Canonical Moments with Applications in Statistics, Probability, and Analysis*, Wiley, New York (1997).

Diemer, R. B., and J. H. Olson, "A Moment Methodology for Coagulation and Breakage Problems: Part II—Moment Models and Distribution Reconstruction," *Chem. Eng. Sci.*, **57**, 2211 (2002).

Gelbard, F., and J. H. Seinfield, "Numerical Solution of Dynamic Equation for Particulate Systems," *J. Comput. Phys.*, **28**, 357 (1978).

Gordon, R. G., "Error Bounds in Equilibrium Statistical Mechanics," *J. Math. Phys.*, **9**, 655 (1968).

Hounslow, M. J., R. L. Ryall, and V. R. Marshall, "A Discretized Population Balance for Nucleation, Growth, and Aggregation," *AIChE J.*, **34**, 1821 (1988).

Hulburt, H. M., and S. Katz, "Some Problems in Particle Technology," *Chem. Eng. Sci.*, **19**, 555 (1964).

Ilievski, D., and M. J. Hounslow, "Agglomeration During Precipitation: II. Mechanism Deduction from Tracer Data," *AIChE J.*, **41**, 525 (1995).

Jung, W. M., S. H. Kang, W. S. Kim, and C. K. Choi, "Particle Morphology of Calcium Carbonate Precipitated by Gas-Liquid Reaction in a Couette-Taylor Reactor," *Chem. Eng. Sci.*, **55**, 733 (2000).

Kim, W. S., and J. M. Tarbell, "Micromixing Effects on Barium Sulfate Precipitation in an MSMPR Reactor," *Chem. Eng. Commun.*, **146**, 33 (1996).

Krutzer, L. L. M., A. J. G. van Diemen, and H. N. Stein, "The Influence of the Type of Flow on the Orthokinetic Coagulation Rate," *J. Colloid Interface Sci.*, **171**, 429 (1995).

Kumar, S., and D. Ramkrishna, "On the Solution of Population Balance Equations by Discretization—I. A Fixed Point Technique," *Chem. Eng. Sci.*, **51**, 1311 (1996a).

Kumar, S., and D. Ramkrishna, "On the Solution of Population Balance Equations by Discretization—II. A Moving Point Technique," *Chem. Eng. Sci.*, **51**, 1333 (1996b).

Litster, J. D., D. J. Smit, and M. J. Hounslow, "Adjustable Discretized Population Balance for Growth and Aggregation," *AIChE J.*, **41**, 591 (1995).

Marchal, P., R. David, J. P. Klein, and J. Villermaux, "Crystallization and Precipitation Engineering—I. An Efficient Method for Solving Population Balance in Crystallization with Agglomeration," *Chem. Eng. Sci.*, **43**, 59 (1988).

Marchisio, D. L., A. A. Barresi, and R. O. Fox, "Simulation of Turbulent Precipitation in a Semi-Batch Taylor-Couette Reactor Using CFD," *AIChE J.*, **47**, 664 (2001).

Marchisio, D. L., A. A. Barresi, and M. Garbero, "Nucleation, Growth and Agglomeration in Barium Sulfate Turbulent Precipitation," *AIChE J.*, **48**, 2039 (2002).

Marchisio, D. L., R. D. Vigil, and R. O. Fox, "Quadrature Method of Moments for Aggregation-Breakage Processes," *J. Colloid Int. Sci.*, **258**, 322 (2003a).

Marchisio, D. L., R. D. Vigil, and R. O. Fox, "Implementation of the Quadrature Method of Moments in CFD Codes for Aggregation-Breakage Problems," *Chem. Eng. Sci.*, in press (2003b).

McGraw, R., "Description of Aerosol Dynamics by the Quadrature Method of Moments," *Aerosol Sci. Tech.*, **27**, 255 (1997).

Muhr, H., R. David, and J. Villermaux, "Crystallization and Precipitation Engineering—VI. Solving Population Balance in the Case of the Precipitation of Silver Bromide Crystals with High Primary Nucleation Rates by Using First Order Upwind Differentiation," *Chem. Eng. Sci.*, **51**, 309 (1996).

Pagliolico, S., D. Marchisio, and A. A. Barresi, "Influence of Operating Conditions on $BaSO_4$ Crystal Size Distribution and Morphology in a Continuous Couette Type Precipitator," *J. Ther. Anal. Cal.*, **56**, 1423 (1999).

Piton, D., R. O. Fox, and B. Marcant, "Simulation of Fine Particle Formation by Precipitation by Using Computational Fluid Dynamics," *Can. J. Chem. Eng.*, **78**, 983 (2000).

Press, W. H., S. A. Teukolsky, W. T. Vetterling, and B. P. Flannery, *Numerical Recipes*, Cambridge Univ. Press, Cambridge (1992).

Ramkrishna, D., "The Status of Population Balances," *Rev. Chem. Eng.*, **3**, 49 (1985).

Ramkrishna, D., *Population Balances: Theory and Applications to Particulate Systems in Engineering*, Academic Press, New York (2000).

Randolph, A. D., and M. A. Larson, *Theory of Particulate Process*, 2nd ed., Academic Press, New York (1988).

Smith, M., and T. Matsoukas, "Constant-Number Monte Carlo Simulation of Population Balances," *Chem. Eng. Sci.*, **53**, 1777 (1998).

Smoluchowski, M. Z., "Versuch Einer Mathematischen Theorie Der Koagulationskinetik Kolloider Losunger," *Z. Phys. Chem.*, **92**, 129 (1917).

Sung, M. H., I. S. Choi, J. S. Kim, and W. S. Kim, "Agglomeration of Yttrium Oxalate Particles Produced by Reaction Precipitation in Semi-Batch Reactor," *Chem. Eng. Sci.*, **55**, 2173 (2000).

Vanni, M., "Discretized Procedure for the Breakage Equation," *AIChE J.*, **45**, 916 (1999).

Vanni, M., "Approximate Population Balance Equations for Aggregation-Breakage Processes," *J. Colloid Interface Sci.*, **221**, 143 (2000).

Wright, D. L., R. McGraw, and D. E. Rosner, "Bivariate Extension of the Quadrature Method of Moments for Modeling Simultaneous Coagulation and Sintering Particle Populations," *J. Colloid Interface Sci.*, **236**, 242 (2001).

Zauner, R., and A. G. Jones, "Determination of Nucleation, Growth, Agglomeration and Disruption Kinetics from Experimental Precipitation Data: the Calcium Oxalated System," *Chem. Eng. Sci.*, **55**, 4219 (2000).

Manuscript received Jan. 28, 2002, and revision received Dec. 9, 2002.